Supporting Information

Title: In-vivo actuation of compliant dielectric elastomer artificial muscles via a peripheral nerve interface.

Stefania Konstantinidi et al.

Text S1. Animal model choice

Rats were chosen as the initial in-vivo model to demonstrate the functionality of rDEAs due to their practical size, ease of handling, and well-characterized anatomy. Subcutaneous implantation is feasible, allowing precise monitoring of actuator-induced displacements using laser sensors. The sciatic nerve provides an accessible site for neural interfacing and real-time control of the actuators. While the rat facial anatomy does not fully replicate human facial muscles, the tissue mechanics and implant environment provide a relevant and reproducible platform for proof-of-concept testing. This approach enables initial validation of actuator performance and neural control in living tissue, forming a foundation for future studies in larger animal models more closely approximating human anatomy.

Text S2. Fabrication process of the reinforced actuators

The fabrication process includes laser cutting of the masks, electrode mixture preparation, stencil printing of compliant electrodes, dielectric film deposition, curing and stacking, followed by fiber alignment and deposition. The full sequence is illustrated in Fig. S1 and detailed in the *Materials and Methods* section. Each actuator layer consists of a 100 µm Elastosil film sandwiched between carbon-based electrodes, encapsulated in a 20 µm silicone layer for insulation and protection.

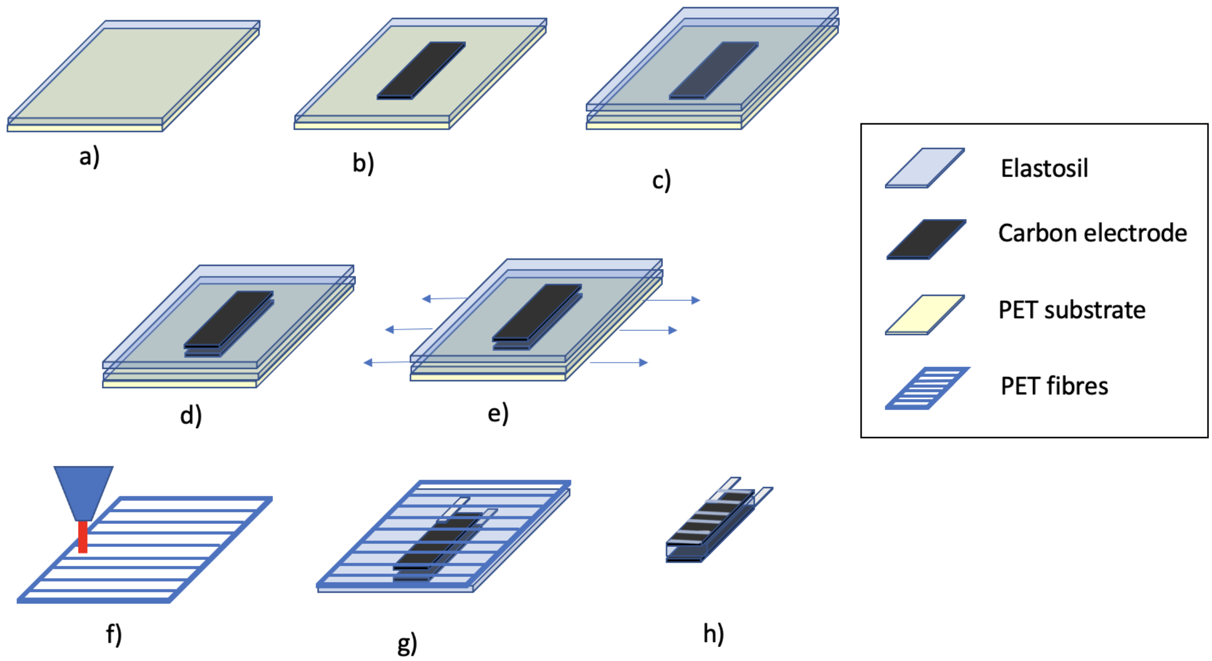

Fig. S1.

Schematics of the fabrication process. a) Elastosil silicone film. b) Stencil printing of the first electrode. c) Deposition of dielectric elastosil film. d) Stencil printing of the second electrode. e) Optional pre-stretching of the actuator. f) Laser cutting the layer sheet into the desired fiber shape. g) Gluing of the fibers onto the DEA and silicone encapsulation application. h) Removing of the PET substrate and cutting the resulting DEA.

Text S2. Caracterisation of the actuators

Mechanical and electromechanical characterization was performed using a pull-tester (Fig. S2) equipped with a high-voltage amplifier and a laser displacement sensor. Actuators were cyclically loaded (stretch ratio 1.0–1.25) under voltages up to 8 kV. Reinforced samples were oriented with fibers transverse to the stretching direction. Figs S3-S6 describe the actuator's behaviour.

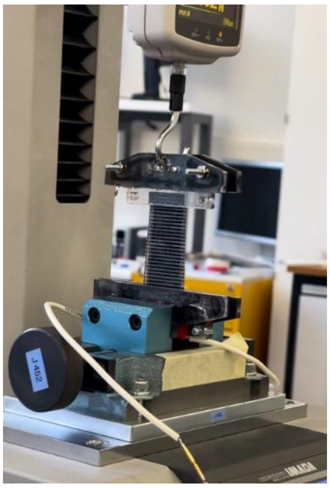

Fig. S2.

Pull-tester setup for the mechanical characterization of the actuators.

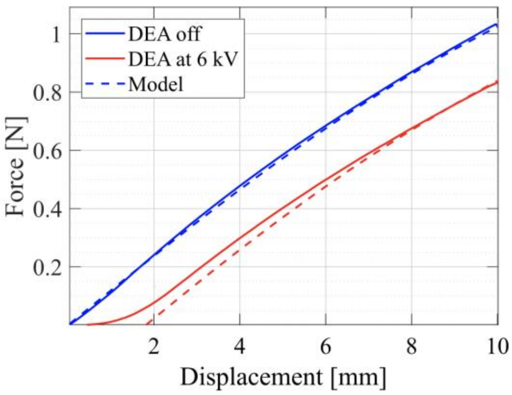

Fig. S3.

Force-displacement characteristic for fiber reinforced DEA operated at 6 kVs with PET fibers and comparison with the model predictions.

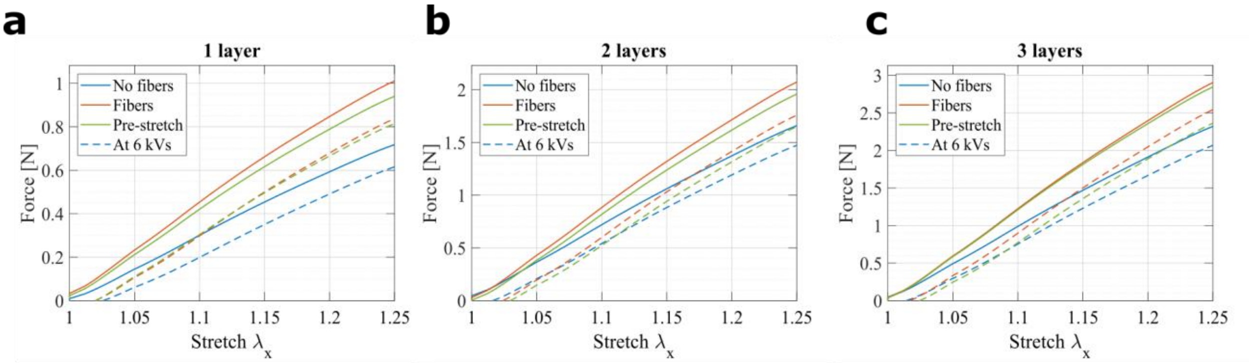

Fig. S4.

Force–stretch characteristics for actuators at rest and actuated at 6 kV, comparing configurations without fibers, with fibers, and with pre-stretch: (a) one layer, (b) two layers, (c) three layers.

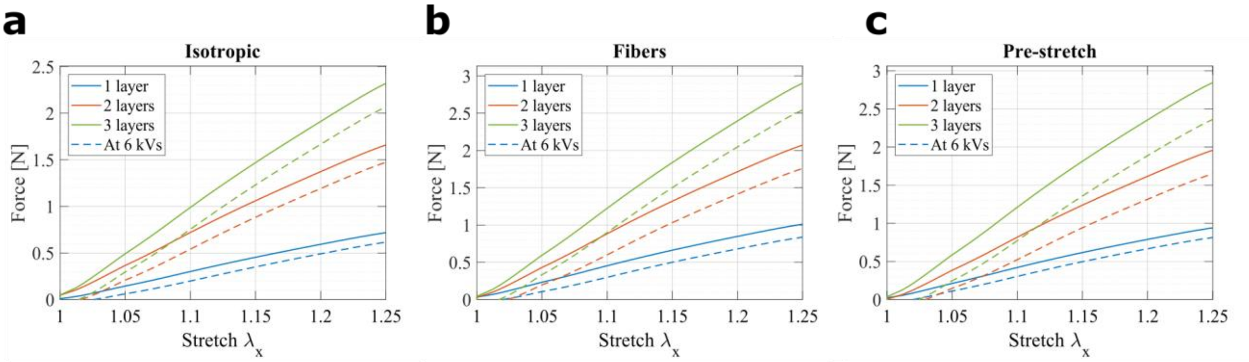

Fig. S5.

Force–stretch characteristics comparing the number of active layers for (a) isotropic actuators, (b) reinforced actuators, and (c) pre-stretched reinforced actuators.

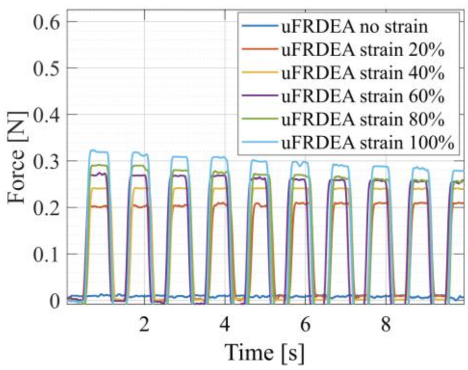

Fig. S6.

Step force recordings for a reinforced DEA with PET fibers operated at 6 kVs with different strains in the direction perpendicular to the fibers (1 layer actuator).

<u>Text S3. Encapsulation of the actuators</u>

Encapsulation ensures mechanical protection and electrical insulation. The top silicone layer (20 µm) is applied over the actuator and cured. Additional silicone was added around the connections of the DEA to avoid short circuit of the conductive areas. Encapsulated actuators were immersed in water (Fig. S7) for preliminary durability testing, confirming no short circuits or delamination occurred.

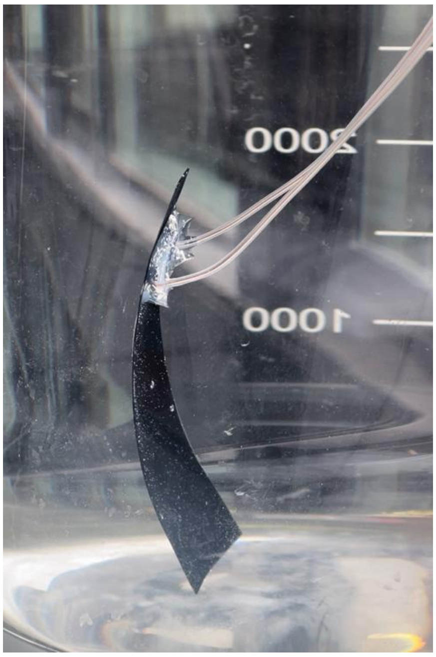

Fig. S7.
Encapsulated DEA connections with silicone and underwater testing.

Text S2. In-vitro surrogate skin

Silicone-based surrogate tissues were prepared to mimic mechanical properties of rat and human skin. PMMA molds were laser-cut, and LSR4305 silicone was poured and degassed in a vacuum chamber before curing at 80 °C for 2 h (Fig. S8). Mechanical testing confirmed linear force-displacement behavior as shown in Fig. S9, with displacement of 6.95 mm for 2 N, corresponding to the specifications.

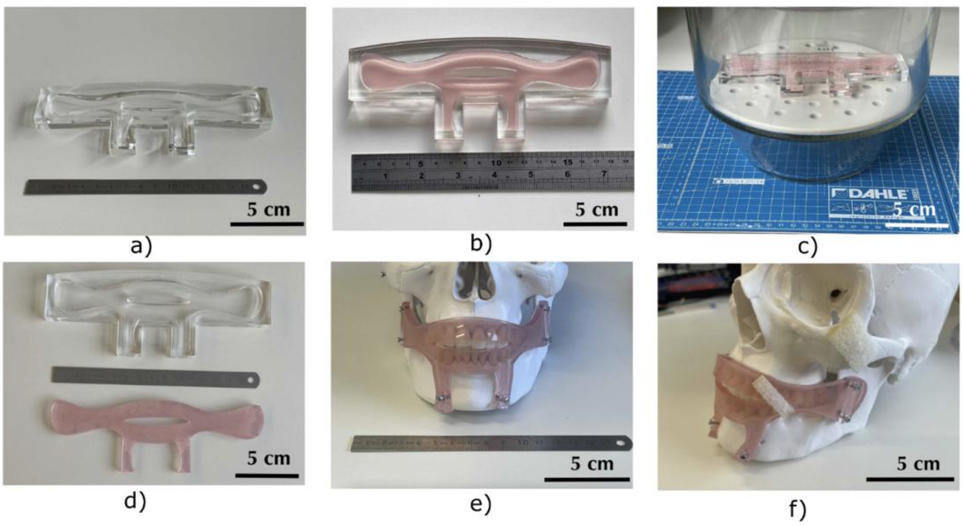

Fig. S8.

Fabrication steps for the surrogate tissue and assembly of the setup. a) Laser cut mold. b) Pouring of the silicone into the mold. c) Vacuum chamber to remove air bubbles from the silone. d) Unmolding of the silicone after thermal curing. e) Assembly of the passive muscles onto the skull. f) Velcro attachments are mounted onto the silicone and the skull to allow the attachment of the DEA.

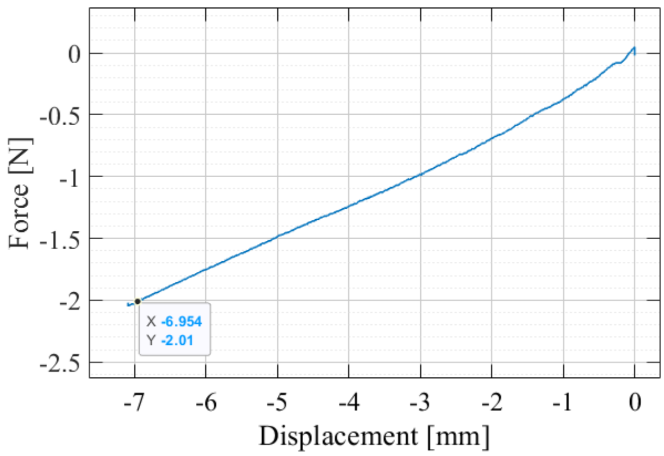

Fig. S9.

Surrogate tissue mechanical testing, force-displacement curve.

Text S4. Experimental and surgical setup

A computer is used to monitor and process the sciatic nerve electrode signal, which is used to operate the DEA through a high voltage (HV) power supply. The displacement is monitored using a camera placed on top of the rat and a laser displacement sensor pointing at a marker.

Text S5. Cadaver testing

Preliminary cadaver experiments were performed to optimize implant placement, attachment sites, and laser sensor positioning as shown in Figs. S11-S14.

Fig. S10.
Sciatic nerve for the cuff electrode placement.

Fig. S11.
Subcutaneous pocket and stitching placement for the attachments at the back of the spine.

Fig. S12.
Attachment sites and actuator fixation on the cadaver specimen, with one end of the actuator attached on the skin of the rat.

Fig. S13.
Closed rat cadaver with the actuator stretched under its skin.

Text S7. Cuff electrodes design and preliminary testing

Prior to *in-vivo* use, all cuff electrodes were functionally verified through electrical and visual testing to ensure proper insulation and contact integrity. Each cuff consisted of a medical-grade silicone tube embedding stranded platinum–iridium contacts. Stimulation and recording performance were assessed under saline using a differential configuration (recording from one ring versus ground).

Functional test: Stimulation was performed in saline, starting at 50 µA and increased gradually; the final amplitude was set ~20% above the activation threshold. Recording was done differentially (one ring vs. ground) and paused during stimulation to avoid artifacts.

Bubble test: Each electrode was immersed in saline and connected to a 6–9 V DC source (negative lead on the contact, positive on a grounded bowl). Single, localized bubbles confirmed proper function; multiple streams indicated a short circuit.

Impedance test: Contact impedance was measured at 1 kHz before and after implantation. Acceptable values ranged from 2–5 kΩ; values > 100 kΩ or < 50 Ω suggested faulty connections.

Sterilization: Cuffs were gas-sterilized and left to outgas for > 48 h, or alternatively rinsed in 70% ethanol and air-dried. Cuffs were moistened with saline prior to implantation to maintain contact stability.

Table S1.
Specifications of the zygomaticus major muscle.

Property		Value	Units
Displacement	Average smile	0.7	cm
Shape	Zygomaticus major	Band, fan or bifid	
Dimensions	Thickness	1	cm
	Width	2	cm
	Length	6	cm

Table S2.
Model parameters.

Parameter	Description	Value	Unit
C10	Yeoh coefficient 1	178426	Pa
C20	Yeoh coefficient 2	-6023	Pa
C30	Yeoh coefficient 3	4234	Pa
Hp	Passive layer's thickness	100	µm
L	Actuator length	25	mm
vf	Fiber Poisson's ratio	0.3	-
H	Dielectric layer thickness	100	µm
wf	Fiber width	1	mm
hf	Fiber thickness	125	µm
Ef	Fiber Young's modulus	2.5	GPa

Table S3.
Body data and anesthetic parameters for tested rats.

Animal ID	Sex	Body weight	Analgesia dosage	Anesthesia dosage	Body temperature
R1	Male	410 grams	1 µl/g	2.5%-2%	33°C
R2	Male	417 grams	1 µl/g	1.8%-1.5%	34°C
R3	Female	331 grams	1 µl/g	1.8%-2%	34°C
R4	Female	293 grams	1 µl/g	1.8%-2%	34°C

Movie S1. In-vivo actuation of rDEA under direct voltage control.

Movie S2. Neural-controlled actuation using sciatic nerve signals.

Movie S3. In-vitro setup and actuation.